

2019-03-07

The distribution of deep-sea sponge aggregations (Porifera) in relation to oceanographic processes in the Faroe-Shetland Channel.

Davison, J

<http://hdl.handle.net/10026.1/13461>

10.1016/j.dsr.2019.03.005

Deep Sea Research Part I: Oceanographic Research Papers

Elsevier

All content in PEARL is protected by copyright law. Author manuscripts are made available in accordance with publisher policies. Please cite only the published version using the details provided on the item record or document. In the absence of an open licence (e.g. Creative Commons), permissions for further reuse of content should be sought from the publisher or author.

Highlights

Deep-sea sponge aggregation occurs in area of greatest variation in temperature

There is a log-linear relationship between sponge abundance and temperature variability

Temperature variability is attributed to internal wave activity in the study area

Sponge abundance is related to long term (132 days) mean suspended particulate matter

1 The distribution of deep-sea sponge aggregations (Porifera) in relation to oceanographic processes in
2 the Faroe-Shetland Channel.

3 Joshua J. Davison¹, Hans van Haren², Phil Hosegood¹, Nils Piechaud¹,*Kerry L. Howell¹,

4

5 ¹Marine Institute, Plymouth University, Plymouth, PL4 8AA, UK.

6 ²Royal Netherlands Institute of Sea Research (NIOZ) and Utrecht University, Den Burg, the
7 Netherlands.

8

9 Correspondence author's name:

10 Kerry Howell, email: Kerry.Howell@plymouth.ac.uk

11

12 Key words: internal waves; Porifera; sponge aggregations; deep-sea; marine conservation;

13

14 Abstract:

15 Deep-sea sponge aggregations have been identified as potential Vulnerable Marine Ecosystems under
16 United Nations General Assembly Resolution 61/105. Understanding the distribution of these habitats
17 is critical to future spatial management efforts, and central to this understanding are quantitative data
18 on the environmental drivers of that distribution. Accumulations of large suspension feeders are
19 hypothesised to aggregate in regions of internal wave formation. The causal link is thought to be an
20 increase in the supply of food related to the incidence of internal waves, which results in resuspension
21 of particulate organic matter on which the sponges feed. There is, however, almost no empirical
22 evidence to support this hypothesis for deep-sea sponge aggregations, although there is strong
23 circumstantial evidence. We tested the relationship between sponge density and 1) temperature range
24 (as a measure of internal wave presence in this region), and 2) optical backscatter (a measure of
25 particulate flux) for a known sponge aggregation in the Faroe-Shetland Channel where internal wave
26 interaction with the slope is further well-documented. 25 benthic video transects, ranging from 422-
27 979m water depth were conducted in the study region. 225 images were analysed and all taxa
28 identified to morphotypes and quantified. Temperature and optical backscatter data were drawn from
29 archived CTD data, and data from long term (4 months) and 2 seasonal short term (11 days) mooring
30 deployments from the region. A generalised linear model was used to test the relationship between
31 sponge density and temperature range (ΔT), and sponge density and optical backscatter. The results
32 showed a statistically significant positive relationship between sponge density and temperature range,
33 with the highest sponge densities occurring at depths of greatest temperature range. They showed a
34 statistically significant positive relationship between sponge density and optical backscatter for long
35 term and one short term seasonal deployment (Sep-Oct), but a weak negative relationship for the other
36 short term mooring deployment (April-May). We conclude that sponge aggregations in the Faroe-
37 Shetland Channel are associated with slope regions that are subjected to abrupt and pronounced
38 changes in temperature due to intensified internal wave activity over the slope between depths of 400-
39 600 and that lead to intensified near-bed currents and elevated resuspension of particulate. Our data
40 provide empirical evidence of the relationship between internal wave processes and deep-sea sponge

41 aggregations. These data modify current theory on drivers of deep sea sponge aggregation
42 distribution, suggesting aggregations also occur directly within regions of internal wave breaking,
43 rather than simply proximal to these regions.

44

45 1. Introduction

46 Deep-sea sponge aggregations are communities of large sponges that form under specific biological,
47 hydrological and geological conditions (Hogg *et al.*, 2010). They are a global phenomenon (Van Soest
48 *et al.*, 2012), examples of which include: *Pheronema* (formerly known as *Holtenia*) grounds
49 characterised by *Pheronema carpenteri* (Thomson, 1869) in the NE Atlantic (Rice *et al.*, 1990), dense
50 Hexactinellid reefs found off the coast of British Columbia, Canada (Krautter *et al.*, 2001) and ostur
51 grounds characterised by large demosponges on the Faroese slope and shelf (Klitgaard & Tendal,
52 2004; Murillo *et al.*, 2018). Deep-sea sponge aggregations have been identified as potential
53 Vulnerable Marine Ecosystems (VME) (UNGA Res. 61/105) under the FAO's guidelines for the
54 management of deep-sea fisheries (FAO, 2009), and are listed under the OSPAR Convention as a
55 threatened and declining habitat (OSPAR, 2010). Furthermore, a recent Convention on Biological
56 Diversity (CBD) Decision XX/4 emphasised the ecological importance and sensitivity of these
57 aggregations and the need to study and conserve them; and the United Nations Environment
58 Programme have called for international engagement in mapping and modelling sponge distribution
59 (Hogg *et al.*, 2010).

60 Effective management and conservation of these habitats relies on a firm understanding of
61 their spatial distribution. While there are a number of growing datasets on the presence of individual
62 sponge taxa, data on the presence of sponge aggregations is limited, and so recent studies have
63 attempted to predict their distribution using habitat suitability modelling approaches (Knudby *et al.*,
64 2013; Ross & Howell, 2013; Howell *et al.*, 2016). The construction of models requires data on the
65 presence / absence / abundance of a species and spatial layers of data on relevant environmental
66 parameters. Models can then be developed that formalise the relationship between species presence /

67 absence / abundance and the environmental drivers (or surrogates for those drivers) of their
68 distribution within a statistical framework. However, questions remain around the accuracy and
69 reliability of modelled maps, particularly where there is only a very basic understanding of the
70 underlying ecology and environmental drivers of species distributions (Howell *et al.*, 2016).

71 The distribution of deep-sea sponge aggregations is thought to be related to the interaction of
72 internal waves (IWs) with sloping boundaries, typically the continental slope (Rice *et al.*, 1990;
73 Kittgaard *et al.*, 1997; White, 2003) and raised features like the Mid-Atlantic Ridge (van Haren *et al.*,
74 2017). Rice *et al.* (1990) postulated that accumulations of hexactinellid sponges in the Porcupine
75 Seabight (NE Atlantic) aggregated near regions with a critical slope where the bottom slope matches
76 the slope of propagation of internal tidal waves and near-bed currents are intensified. The causal link
77 was suggested to be an increase in the supply of food related to the occurrence of the internal waves.
78 Sponges are filter-feeders and represent an important link between carbon in the water column in the
79 form of ultraplankton (2-20 μ m) and picoplankton (<2 μ m) (Reiswig, 1975), dissolved organic carbon
80 (Yahel *et al.*, 2003; de Goeij *et al.*, 2008) and potentially viral particles (Hadas *et al.*, 2006), and the
81 benthos. Rice *et al.*'s hypothesis was extended by Klitgaard *et al.* (1997) for aggregations
82 characterised by the demosponge *Geodia* spp, who put forward two mechanisms by which food
83 availability in the form of suspended material might be increased: 1) increased primary production
84 where internal wave mixing promotes nutrient flux to the surface, and 2) leakage of food-particle rich
85 water from the bottom-mixed layer to the stratified ocean interior. To date there has been no formal
86 testing of this hypothesis.

87 Within the Faroe-Shetland Channel (FSC) sponge aggregations are known to occur on shelf
88 areas around the Faroe Islands (Klitgaard & Tendal, 2004) as well as on the continental slope west of
89 the Shetland Islands (Bett, 2001). These sponge aggregations have been classified as 'Boreal Ostur'
90 (Klitgaard & Tendal, 2004). They are characterised by sponges of the genus *Geodia*, specifically
91 *Geodia barretti* (Bowerbank 1858), *G. macandrewi* (Bowerbank 1858), *G. atlantica* (Stephens, 1915)
92 and *G. phlegraei* (Sollas 1880).

93 The FSC is also a site with particularly intense IW processes (Van Raaphorst *et al.*, 2001;
94 Hosegood *et al.*, 2004) that result in dramatic short-term changes in temperature (Hosegood, 2004a,
95 b). In addition to the generation of internal tides at a semidiurnal frequency throughout the channel
96 (Hosegood & van Haren, 2006; Hall *et al.*, 2011), resuspension may be promoted by the propagation
97 of ‘solibores’ up the continental slope. Defined as features that resemble both internal bores and
98 nonlinear internal wave trains, solibores have been observed to generate a temperature decrease of
99 $>4^{\circ}\text{C}$ in less than one minute at a depth of 470 m. In the FSC, particulate fluxes are two orders of
100 magnitude larger than background levels for 2 days following the passage of solibores (Hosegood *et*
101 *al.*, 2004a). Key to their generation, and the continuous critical reflection of the internal tide over the
102 slope that occurs further to the south in the FSC and generates similar near-bed intensified currents
103 (Hall *et al.*, 2011), is the intersection of the strongly stratified permanent pycnocline over the Shetland
104 slope at depths of 400-600 m. Separating the poleward flowing surface waters of Atlantic origin and
105 the equatorward flowing waters of polar origin, the pycnocline persistently renders the slope critical to
106 internal wave reflection at the depth where it intersects the bottom, but whose location varies over
107 time due to tidal, and lower frequency, modulations of the current regime (Hosegood & van Haren,
108 2006).

109 Within the depth range of 400-600 m in the FSC, resuspension of particulate material is thus
110 persistently driven by the internal tide whereby near-bed currents and temporal changes in
111 temperature are bottom intensified with a semidiurnal frequency. Due to changes in background
112 stratification, the signature of such resuspension in moored OBS signals is effectively switched on and
113 off at a given location due to the location of internal tide generation (Bonnin *et al.*, 2002); as the
114 background stratification evolves in response to regional scale, subinertial forcing such as coastal
115 trapped waves (Hosegood *et al.*, 2006), the precise depth at which the slope is critical to the
116 semidiurnal internal tide changes within the 400-600 m range (Hosegood & van Haren, 2006). The
117 FSC has thus long been a site of multidisciplinary study due to these unique biological and
118 hydrographic characteristics and is an excellent site for investigating relationships between IW
119 processes and sponge aggregations.

120 Whilst the association between ostur aggregations in this region and IW processes has been
121 suggested by previous authors (Bett, 2001; Klitgaard & Tendal, 2004), there has been no robust
122 analysis of these relationships. This study aims to consolidate our understanding of the role of IW in
123 driving the distribution of ostur in the FSC, contributing to the development of more complex habitat
124 suitability models and a deeper understanding of how this valuable and threatened ecosystem is
125 generated and sustained. Our hypotheses are: H1 – The abundance of sponges is associated with the
126 generation of internal waves at the slope, H2 – The abundance of sponges is related to the amount of
127 particulate matter in suspension.

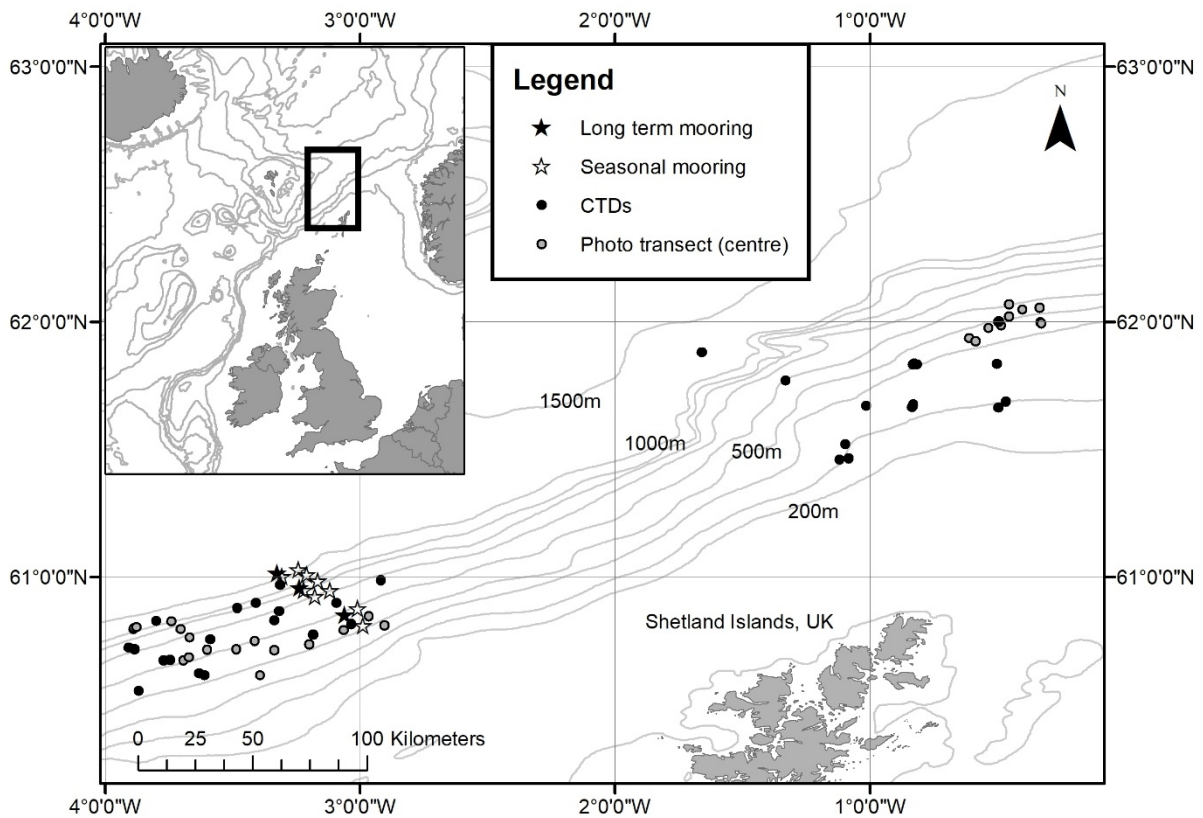
128

129 2. Methods

130 2.1 Study Area

131 The FSC is a roughly symmetrical, widening trench bounded by the Faroe Islands in the west and the
132 Shetland Islands in the east (Fig. 1). It has a roughly southwest to northeast orientation. In the
133 southwest the channel terminates in sills at a depth of 850m and 500m at the Faroe Bank Channel and
134 Wyville-Thomson Ridge, respectively. To the Northeast the FSC meets the Norwegian Sea at between
135 1500-2000m (Van Raaphorst *et al.*, 2001). The hydrography of the FSC is primarily underpinned by
136 the constituents of the water column, which comprises 5 distinct water masses described in Turrell *et*
137 *al.* (1999).

138



139

140 Figure 1: Map of the Faroe-Shetland Channel detailing the locations of areas of study, CTD casts,
 141 image transects (mid point shown), and PROCS-1-3 mooring sites, North of Scotland, Shetland and
 142 Orkney shown in grey.

143

144 2.2 Biological Data

145 Biological data were derived from 25 benthic video / image transects conducted by the M/V Franklin
 146 during the combined Strategic Environment Assessment 7/ Special Area for Conservation survey in
 147 2006 (Jacobs & Howell, 2007). Transects were conducted on two separate sites; FSC_NE ($n=9$)
 148 ($62^{\circ}00-00'N$, $1^{\circ}00-00'W$) and FSC_SW ($n=16$) ($61^{\circ}00-00'N$, $3^{\circ}30-00'W$) (Fig. 1) and ranged from
 149 473m to 2591m in length. Sea-floor image data were collected with the SEATRONICS drop frame
 150 camera system (Howell *et al.*, 2010). The system comprised an integrated DTS 6000 digital video
 151 telemetry system, which provided a real time video link to the surface, a digital stills camera (5 mega
 152 pixel, Kongsberg OE14-208) and a colour video camera (Kongsberg OE14-366). The stills camera

153 was mounted at an oblique angle (22°) to the seabed. Sensors monitored depth, altitude and
154 temperature, and an Ultra Short Base Line (USBL) beacon provided position data accurate to 1m
155 (Howell et al., 2007). The drop frame was towed in the water column between one and three metres
156 above the seabed. At approximately 1 minute intervals the camera was landed on the seabed and a still
157 image taken. This ensured a consistent size field of view for images.

158 For each transect 9 images were quasi-randomly selected for analysis, giving 225 images for analysis.
159 Compromised images (e.g. high sediment, large obstructions, resolution or contrast issues) were
160 omitted and an alternative image selected. Selected images were quantitatively analysed in the
161 following manner: all sponges $>1\text{cm}$ were identified and counted, percentage cover of sponges was
162 also calculated using a calibrated grid superimposed over the image (data were rounded to the nearest
163 0.25 of a grid square). Sponge taxa were identified as distinct Operational Taxonomic Units (OTUs)
164 following Howell & Davies (2010). OTUs may not conform to established taxonomy. Sponge OTUs
165 were defined by colour, shape, and specific terminology found within Ackers *et al.* (2007) and
166 grouped into distinct morphologically similar groups as a result of the difficulty in identifying
167 sponges using images. Image data were then pooled by transect.

168

169 2.3 Oceanographic Data

170 Variation in the temperature range with depth was chosen as an indicator for the presence of internal
171 waves at the seabed as recorded by Nansen (1902). Archived CTD casts for the immediate region of
172 study (FSC_NE = 18n, FSC_SW = 18n) were obtained from the British Oceanographic Data Centre
173 (BODC) (Fig. 1). The CTD profiles all reach to within approximately 10 m of the sea bed. These data
174 spanned a period of 28 years (1984-2012). Mean, range and standard deviation were calculated for
175 temperature ($^\circ\text{C}$) at 20m depth intervals from all CTD casts ($n=36$) from 0-1300m (Supplementary
176 material, Fig. S1). These data are considered low temporal resolution data and will be referred to as
177 such henceforth.

178

179 Higher resolution data on temperature, and data on turbidity (optical back scatter, (OBS)) were
180 obtained from moorings deployed over the Shetland continental slope by the Royal Netherlands
181 Institute of Sea Research (NIOZ) during the ‘Processes on the Continental Slope’ (PROCS)
182 programme (Fig. 1). Medium temporal resolution data (hereinafter referred to as PROCS-2 data) were
183 derived from three ‘long term’ moorings deployed for a period of 132 days (May – Sept 1999) at 552,
184 803, 1043m depth. Temperature and optical backscatter were recorded hourly. In addition seasonal
185 high temporal resolution data were obtained from two further sets of moorings deployed for an 11 day
186 period in April-May (PROCS-1 research cruise, 4 moorings at 471, 700, 777, 1000m) and Sept-Oct
187 (PROCS-3 research cruise, 5 moorings at 550, 700, 800, 900, 1000m) (Fig. 2). Temperature and
188 optical back scatter was logged every 4 mins.

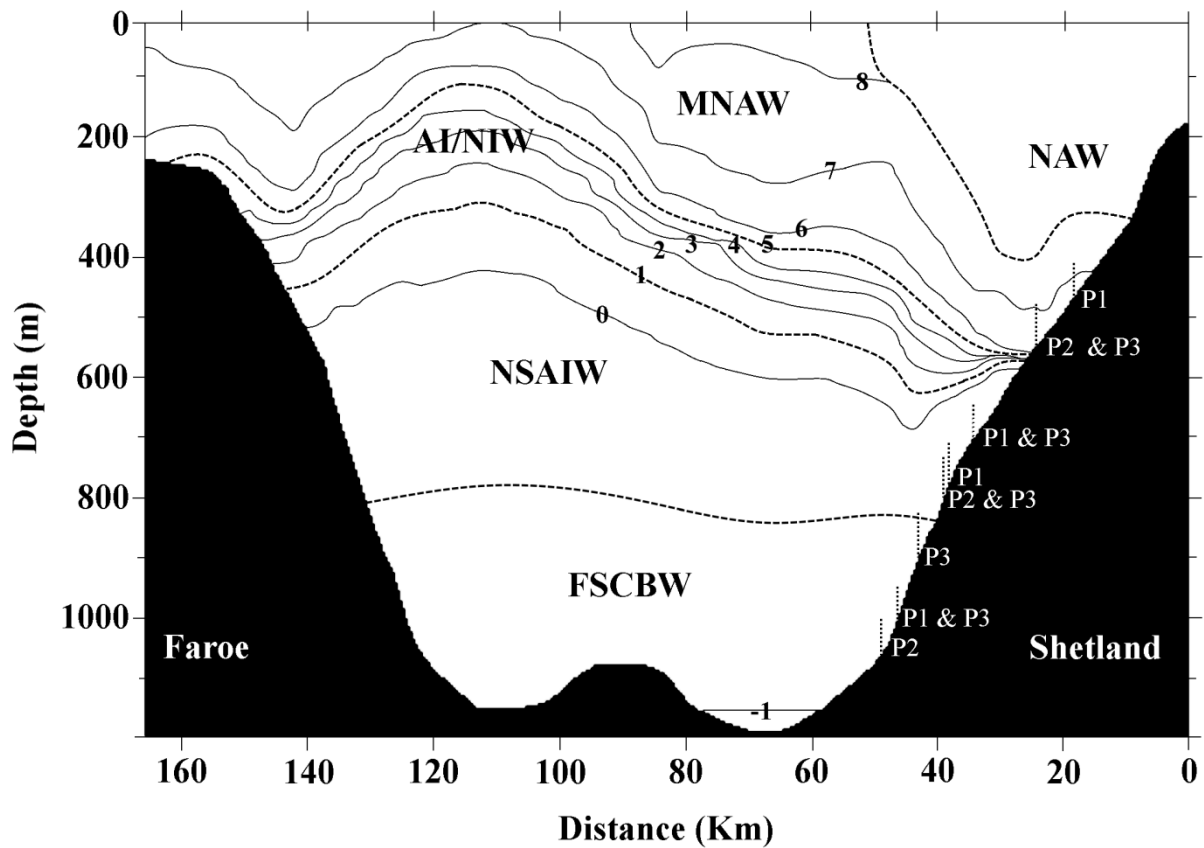
189

190 Optical backscatter was measured using a Seapoint STM optical backscatter sensor (OBS). Optical
191 backscatter indicates the presence of suspended particulate matter with the limitation that the raw
192 signal (measured in Volts, with a higher voltage indicating a greater proportion of suspended
193 particles) depends heavily on the particle size in accordance with Bunt et al., (1999), who found that
194 optical devices are most sensitive to particles <20µm in diameter. The OBS in this study is capable of
195 detecting particles in the ultra and picoplankton size range (size fraction on plankton known to be
196 utilised by sponges as a food resource), but it must be noted that OBS is a bulk measure of suspended
197 material and its use here as a proxy for availability of potential food resource for sponges is limited
198 and this is acknowledged in the discussion.

199

200 For medium and high resolution moorings data mean, range and standard deviation were calculated
201 for temperature (°C) and OBS over the full deployment period for each mooring. To investigate the
202 relationship between sponge abundance and temperature variation / OBS, each photo transect was
203 paired with the nearest mooring from each of the PROCS1, PROCS2 and PROCS3 datasets.

204



205

206 Figure 2: Cross section of the Faroe-Shetland Channel showing detailed temperature and water
 207 masses as described by Turrell et al. (1999). PROCS-1-3 (P1-3) mooring depths are indicated by
 208 vertical dashed lines. Numbers 0-8 are isotherms in °C; water masses are North Atlantic Water,
 209 Modified North Atlantic Water, Arctic Intermediate / North Icelandic Water, Norwegian Sea Arctic
 210 Intermediate Water, Faroe-Shetland Channel Bottom Water (Redrawn from Hosegood, 2005).

211

212 2.4 Statistical Analysis

213 Preliminary analysis demonstrated that temperature range data (ΔT) from CTDs, long term and short
 214 term moorings were highly correlated therefore only CTD data were used in further analyses. In
 215 addition, sponge abundance and sponge percent cover were highly correlated (Kendall's Rank (Tau) T
 216 = 0.646, $P < 0.001$) and so only sponge abundance was used in further analyses. Scatter plots of sponge
 217 abundance vs temperature range suggested a log-linear or polynomial relationship was present.
 218 Simple linear, log linear and polynomial models were fitted to the data, however a log-linear model

219 provided the best fit and explained substantially more variance than other models trialled. To test H1 a
220 linear model was used to test for a significant relationship between log sponge abundance and ΔT
221 from archived CTD data.

222 Scatter plots of sponge abundance vs OBS again suggested a log-linear or polynomial relationship
223 was present between sponge abundance and OBS. However, the limited data available for OBS from
224 only 3 or 4 moorings (depending on whether long term or seasonal datasets) meant it was inappropriate
225 to fit a model to these datasets. Instead for long term (PROCS-2) data, sponge abundance data were
226 grouped by mooring (OBS) and a Kruskal–Wallis test was used to test for a significant differences
227 in sponge abundance between moorings and thus long term (PROCS-2) OBS data. The relationship
228 between sponge abundance and short term seasonal (PROCS-1 and PROCS-3) OBS data were not
229 formally tested but are described.. Data analysis was conducted using R-Studio (RStudio Team, 2016)
230 a wrapper for the program R (version 3.3.2 (R Core Team, 2016)).

231

232 3. Results

233 3.1 Sponge abundance and variation in temperature (indicative of the influence of internal waves)

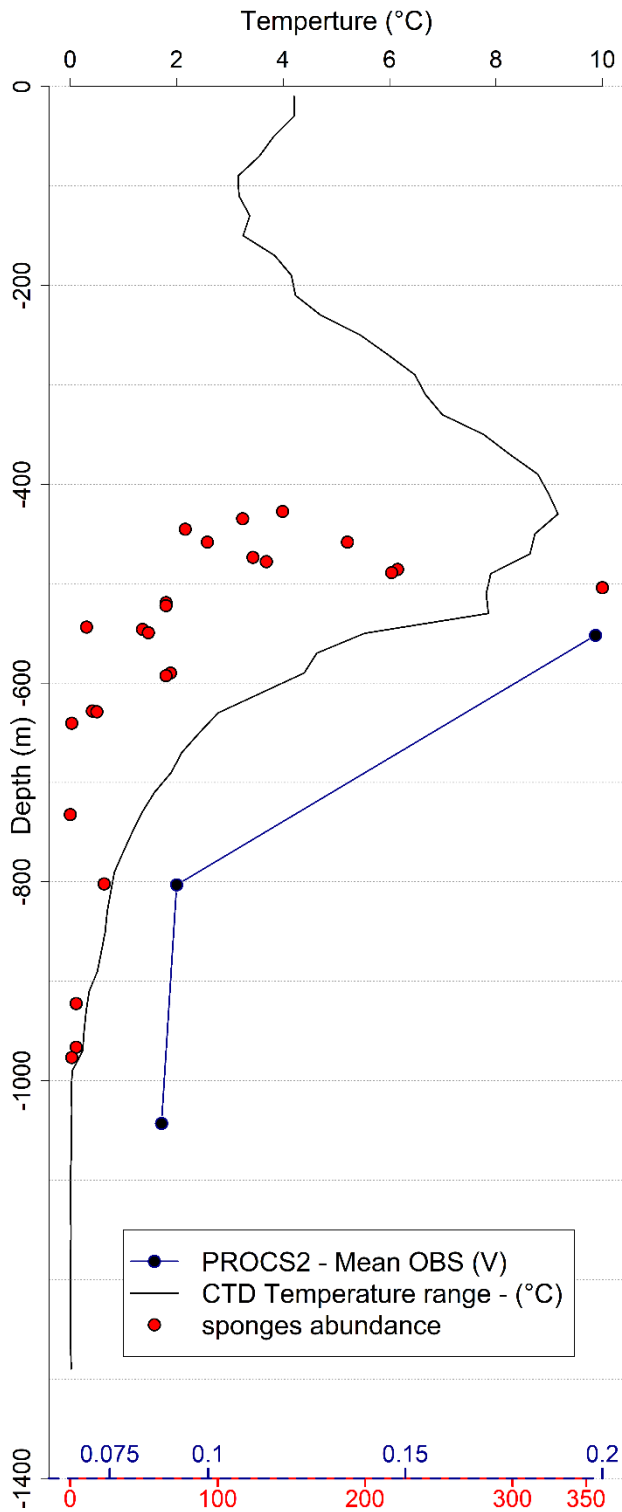
234 ΔT for all datasets peaked between 400 and 600m, with a maximum range of around 9°C (Fig. 3, Fig.
235 S1). Sponge abundance peaked at approximately 500m (498m =361 individuals), and transects with
236 the highest recorded abundances were all located between ~400-600m (Fig. 3). Sponge abundance
237 declines rapidly deeper than 600m. There is a highly significant linear relationship between log
238 sponge abundance and ΔT ($p < 0.001$, Multiple R-squared: 0.73 on 23 df, Supplementary material,
239 Fig. S2).

240 3.2 Sponge abundance and the resuspension of particulate material

241 Box plots of mean long term OBS data (PROCS-2) appeared to show a log-linear relationship with
242 sponge abundance although this was not formally tested as a result of limited data. A Kruskal–Wallis
243 test confirmed there was a significant difference in sponge abundance between moorings and
244 therefore low, medium, and high OBS values (p -value = 0.01238). These data suggest that sponge

245 abundance is related to mean long term particulate resuspension at the seabed (Fig. 3) However, the
246 data are confounded by depth, and have limited resolution as photo transect data have been assigned
247 to the nearest mooring, and data are only available from 3 moorings (Supplementary material Fig.
248 S3). High resolution seasonal data for Sept-Oct (PROCS-3) appeared to have a positive log-linear
249 relationship with sponge abundance, however seasonal data for April-May (PROCS-1) showed a
250 more complex relationship with sponge abundance, where sponges abundance was low at very high
251 OBS values (Supplementary material Fig. S4). This suggests that sponge abundance has a more
252 complex relationship with short term seasonal observations of OBS. However, again it must be
253 considered that data are only available from 4 moorings.

254



255

256 Figure 3: Sponge abundance determined from pooled image data by transect, temperature variation

257 (ΔT) from CTD casts, and long term optical backscatter (PROCS-2) as a function of depth.

258

259

260 4. Discussion

261 4.1 Sponge abundance and temperature variations

262 Large temperature changes are observed between 400-600m depth in this region of the FSC which, on
263 the basis of previous studies, are attributed to internal wave activity (Fig. 3). This depth-range is
264 consistent with the established critical slope angle for internal semi-diurnal tidal waves (M_2 waves),
265 calculated to be 350-550m on the SE slope of the FSC (Van Raaphorst *et al.*, 2001) but also the depth
266 range over which solibores propagate up, and along, the slope (Hosegood *et al.*, 2004b). The highest
267 densities of sponges are also located at between 400-600m, and our results suggest there is a
268 significant linear relationship between temperature range and sponge abundance, suggesting that
269 sponge abundance is highest in the region of internal wave activity at the seabed. The mechanism
270 responsible for the generation of the solibores in this particular location have been suggested to be the
271 nonlinear evolution of the permanent pycnocline that subsequently evolves into various forms of an
272 internal wave train (Hosegood *et al.*, 2006). Internal tides are not necessarily responsible but we note
273 that Hall *et al.* (2011) observed dynamically similar features in the southern prion of the FSC to occur
274 with semidiurnal frequency leading to the conclusion that the critical slopes at this depth range lead to
275 nonlinear internal tide reflection. The common factor in either scenario is a rapid drop in temperature
276 accompanied by intense near-bed currents.

277 Although in general agreement, this is contrary to the current theory, which suggests sponge
278 aggregations are found near to, but not in, regions of internal wave breaking (Rice *et al.*, 1990;
279 Kittgaard *et al.*, 1997; White 2003). Increased velocities associated with regions of critical slope angle
280 and therefore internal wave propagation were postulated to be too severe for sponge species to persist
281 (White, 2003). Sponge aggregations were postulated to form 'downstream' of regions of breaking
282 internal waves, such that they benefitted from material transported by turbulent mixing but were not
283 subject to breaking waves. In this study the highest densities of sponges were found at ~500m (Fig. 3)
284 which corresponds well with the highest cross-slope enhancement of velocity at 502m on the SE shelf
285 of the FSC (Van Raaphorst *et al.*, 2001). This study suggests that ostur aggregations are capable of

286 withstanding strong bottom currents. The initial theory was postulated for aggregations of *P.*
287 *carpenteri*, which grow mainly on fine sediments and weakly anchor themselves via a spicule matt
288 (Rice *et al.*, 1990). Ostur species are characteristically found physically attached to gravel, small
289 cobblestones or hard sediments (Klitgaard & Tendal, 2001). Furthermore, ostur sponges are regularly
290 found to have gravel incorporated into the cortex (Klitgaard & Tendal, 2001), which could enable
291 them to more strongly anchor to the seafloor, allowing them to resist faster current speeds.

292 The flow rate through a sponge is also dictated by the ambient flow (Vogel, 1977). *Geodia barretti*
293 (Bowerbank, 1858), a defining species of ostur grounds, has been shown, in a combination of
294 laboratory and *in situ* conditions, to have pumping rates 6 times slower than shallow water sponges
295 (Kutti *et al.*, 2013), therefore it is possible that if ostur are able to resist higher current regimes this
296 may lead to greater food acquisition. This could be achieved by increased flow through the sponge as
297 a result of the significantly enhanced bottom currents due to internal wave breaking, where peak
298 current velocities in this region can reach $>75\text{cm s}^{-1}$ (Masson, 2001).

299

300 4.2 Sponge abundance and the resuspension of particulate material

301 We found significant differences in sponge abundance between areas of low, medium and high OBS,
302 and our data suggest there may be a positive log-linear relationship between sponge abundance and
303 OBS from long term mooring data as well as seasonal short term mooring data (PROCS-3), although
304 available data were insufficient to formally test this. High OBS values are indicative of high levels of
305 suspended particulate material.

306 Current theory suggests that sponge aggregations are promoted by the presence of internal waves as a
307 result of either: 1) increased primary production that may occur where internal wave mixing promotes
308 nutrient flux to the surface, or 2) leakage of food-particle rich water from the bottom-mixed layer to
309 the stratified ocean interior. Our data would suggest the latter mechanism may operate in the FSC.
310 Due to the presence of tidally driven internal waves (Van Raaphorst *et al.*, 2001; Hosegood *et al.*,
311 2006) and solibores generated by subinertial processes (Hosegood *et al.*, 2004b), there is likely to be a

312 permanent intermediate nepheloid layer between the intermediate and deep water masses (Turrell *et*
313 *al.*, 1999) around 500-550m (Van Raaphorst *et al.*, 2001). This nepheloid layer could provide the
314 sponges with a sustained and reliable food source and thus support the formation of aggregations. A
315 recent study focused on sponge aggregations on the summit of an Arctic seamount also suggested
316 sponge densities were associated with elevated near-bed suspended particulate material
317 concentrations, likely as a result of local / near-field resuspension by tidal currents, the driver being
318 improving food supply to the sponges (Roberts *et al.*, 2018). However, we do not know if the
319 resuspended material observed here is utilised by the sponges as a food source. Nor do we know the
320 nutritional value of the material to the sponge. Thus we cannot demonstrate that it is the resuspension
321 of material that drives sponge abundance through provision of food resource.

322 Although our data suggest a positive log-linear relationship between sponge abundance and OBS data
323 from long term moorings and short term seasonal moorings deployed in Sep-Oct, there is a more
324 complex, relationship between sponge abundance and OBS data from seasonal short term moorings
325 deployed in April-May when the most intense solibores were observed (Hosegood *et al.*, 2004a).

326 Within the April-May short term mooring deployment (PROCS-1) a solibore event occurred on day
327 112 during a barotropic neap tide, the period where internal tidal forcing would be expected to be the
328 weakest (Hosegood *et al.*, 2004b). Solibore events were observed to occur approximately every 4-7
329 days and are not directly associated with tidal forcing (Hosegood *et al.*, 2004b; Hosegood *et al.*,
330 2006), therefore they are not likely to be reliable for frequent particulate resuspension. However,
331 during a solibore event the amount of particulate that can be resuspended is up to 100 times the
332 amount than that can be resuspended by typical steady currents (Fig. S4). During the solibore event
333 observed during PROCS-1 the total max flux at >700m was shown to be 2 orders of magnitude higher
334 than that at 470m during the day following the solibore occurrence (Hosegood *et al.*, 2004a). Sponge
335 abundance is low at 700m where PROCS-1 seasonal OBS is highest (Supplementary material - Figure
336 S4). It is possible that this concentration of particulate matter in the water column might exceed the
337 tolerance levels for the sponges resulting in the clogging of the osculum and ostia, leading to a
338 depressed metabolism and possible mortality (Klitgaard & Tendal, 2004). It is possible that sponge

339 aggregations do not extend deeper in the FSC as a result of these episodic mass flux events. However,
340 geodid sponges are able to tolerate high exposure to suspended particulate by reducing respiration
341 rates by up to 86%, for a short time (Tjensvoll *et al.*, 2013). In addition more recent studies have
342 shown that chronic (29 day) cyclic exposure to natural bottom sediment did not affect geodid
343 respiration (Kutti *et al.*, 2015). It is therefore more likely that the consistently lower temperatures
344 below 600m (~0°C) may lie outside the thermal tolerance of the sponge species observed. Species
345 characteristic of boreal ostur, including *G. barretti*, *G. macandrewi*, *G. atlantica* and *G. phlegraei*,
346 have been observed over a temperature range of -0.62–10.75 °C (Cardenas et al., 2013; Howell et al.,
347 2016), with the lower figures coming from the FSC where the lower temperatures are only
348 experienced periodically not consistently.

349

350 4.3 Further Observations and Remarks

351 This study has shown a significant log-linear relationship between temperature range and sponge
352 abundance, suggesting that sponge abundance is highest in the region of internal wave activity at the
353 seabed. If the relationship between sponge abundance and internal wave processes can be shown to be
354 consistent across multiple sites globally, it would provide a powerful predictor in the further
355 development and application of habitat suitability modelling approaches to predictively map the
356 distribution of sponge aggregations in the deep sea. Our study is of one site in one basin and does not
357 enable such a generalisation to be made. It does however provide quantitative data on the nature of
358 that relationship at this site, such that a more comprehensive test of this relationship can be made in
359 future.

360 This study has also shown that sponge aggregations of the FSC are subjected to rapid and large
361 changes in temperature as result of the extreme thermal gradient in the FSC and the propagation and
362 breaking of internal waves. Sites with sponge aggregations consistently experience 6°C shifts in
363 temperature, with the highest variation being over 9°C (Supplementary material, Fig. S1)).
364 Aggregations are frequently subjected to water <0°C due to the movement of the pycnocline, but

365 temperature varies between approximately -1 and 9°C and is on average around 3.5°C . Changes in
366 temperature of this magnitude might be expected to induce heat shock and possibly mortality. *G.*
367 *barretti*, a key constituent of these aggregations, has been observed to be intolerant to sustained rises
368 in temperature. Guihen *et al.* (2012) observed that 95% of specimens were killed during two heat
369 shock events in 2006 and 2008, by a 4°C rise in temperature in <24h, which was then sustained for
370 several days. Temperatures peaked at 12.6°C. These authors suggested that 12.6°C exceeded the
371 thermal tolerance for *G. barretti* and that observed mortality was caused by microbially induced
372 anaerobic degradation. Our data suggest that *G. barretti* is able to tolerate rapid but sustained
373 fluctuations in temperature of between -1 and 9°C.

374

375 Interestingly a recent study from the Scotian Shelf in the Western Atlantic found that sponge grounds
376 in the Emerald Basin formed by the hexantinellid *Vazella pourtalesi* occurred in areas of historically
377 high inter-annual variability in bottom temperature and salinity (Beazley et al., 2018). Temperature
378 ranged from 4°C in the mid 1960's to upwards of 12°C in more recent years, giving a similar level of
379 shift in temperature (8°C) to that observed in this study over short time-scales. These data suggest that
380 sponge grounds may be tolerant to some level of temperature fluctuation on both short and long-term
381 time-scales. Beazley et al (2018) suggest that these types of observations can give insight into how
382 deep-sea sponge species will respond to future climate change.

383

384 5. Conclusions

385 This paper offers a formal test of the relationship between sponge aggregations and temperature
386 variation (ΔT). Large temperature changes observed between 400-600m depth in this region of the
387 FSC have been attributed to internal wave activity, and this depth-range is consistent with the
388 established critical slope angle for internal semi-diurnal tidal waves (M2 waves). While we cannot
389 rule out the involvement of other oceanographic processes in driving these variations in temperature,
390 available data suggest the abundance of sponges in the FSC is associated with the generation of

391 internal waves at the slope (H1). We have also demonstrated a relationship between sponge
392 abundance and long term (132 days) mean suspended particulate matter in support of H2. The highest
393 values of long term OBS and highest abundance of sponges also occur between 400-600m, where
394 breaking internal waves are known to resuspend particulate material. Formal testing of this
395 relationship is confounded by depth and limited data from only 3 moorings

396

397 6. Acknowledgements

398 The biological data collection was jointly funded by the former UK Department for Trade and
399 Industry (now part of the Department for Business, Innovation and Skills) as part of the UK's
400 Strategic Environmental Assessment 7, and Defra, as part of the Special Area for Conservation
401 surveys. CTD data were obtained from the British Oceanographic Data Centre under NERC open data
402 licences (Open Government License v1.0). Mooring data (temperature, OBS and particulate flux)
403 were collected as part of the PROCS series of cruises funded by the Royal Netherlands Institute of
404 Sea Research (NIOZ). The authors would like to acknowledge with thanks the scientists, officers and
405 crew of MV Franklin and RV Pelagia. We also thank two anonymous reviewers for their helpful
406 comments, and Dr Tony Knights for advice on statistics.

407 References

- 408 Ackers, R.G., Moss, D., Picton, B.E., Stone, S.M.K. & Morrow, C.C., 2007. Sponges of the British
409 Isles (Sponge V). 1992 edition reset with modifications. Marine Conservation Society, Ross-on-Wye.
- 410 Beazley, L., Wang, Z., Kenchington, E., Yashayaev, I., Rapp, H.T., Xavier, J.R., Murillo, F.J.,
411 Fenton, D., Fuller, S., 2018. Predicted distribution of the glass sponge *Vazella pourtalesi* on the
412 Scotian Shelf and its persistence in the face of climatic variability. *PloS One*, 13(10), p.e0205505.
- 413 Bett, B.J., 2001. UK atlantic margin environmental survey: Introduction and overview of bathyal
414 benthic ecology. *Cont. Shelf Res.* 21, 917-956. [https://dx.doi.org/10.1016/S0278-4343\(00\)00119-9](https://dx.doi.org/10.1016/S0278-4343(00)00119-9)
- 415 Bonnin, J., Koning, E., Epping, E., Brummer, G., Brutters, M., 2005. Geochemical characterization of
416 resuspended sediment on the southeast slope of the Faeroe-Shetland Channel. *Mar. Geol.* 214, 215–
417 233. <https://dx.doi.org/10.1016/j.margeo.2004.10.028>
- 418 Bunt, J.A., Larcombe, P., Jago, C.F., 1999. Quantifying the response of optical backscatter devices
419 and transmissometers to variations in suspended particulate matter. *Cont. Shelf Res.* 19, 1199-1220.
- 420 Cardenas, P., Rapp, H.T., Klitgaard, A.B., Best, M., Thollesson, M., Tendal, O.S., 2013. Taxonomy,
421 biogeography and DNA barcodes of *Geodia* species (Porifera, Demospongiae, Tetractinellida) in the
422 Atlantic boreo-arctic region. *Zool. J. Linnean Soc.* 169, 251-311.
- 423 de Goeij, J.M., van den Berg, H., van Oostveen, M.M., Epping, E.H., Van Duyl, F.C., 2008. Major
424 bulk dissolved organic carbon (DOC) removal by encrusting coral reef cavity sponges. *Mar. Ecol.*
425 *Prog. Ser.* 357, 139-151.
- 426 FAO 2009. International guidelines for the management of deep-sea fisheries in the High Seas. 73 p.
427 FAO, Rome.
- 428 Guihen, D., White, M., Lundälv, T., 2012. Temperature shocks and ecological implications at a cold-
429 water coral reef. *Mar. Biodivers. Rec.* 5, 1–10. <https://doi.org/10.1017/S1755267212000413>

430 Hadas, E., Marie, D., Shpigel, M., Ilan, M., 2006. Virus predation by sponges is a new nutrient-flow
431 pathway in coral reef food webs. *Limnol. Oceanogr.* 51, 1548-1550.

432 Hall, R., Huthnance, J., Williams, R., 2011. Internal tides, nonlinear internal wave trains, and mixing
433 in the Faroe-Shetland Channel. *J. Geophys. Res.*, 116, C03008, doi:10.1029/2010JC006213

434 Hogg, M.M., Tendal, O.S., Conway, K.W., Pomponi, S.A., van Soest, R.W.M., Gutt, J., Krautter, M.,
435 Roberts, J.M., 2010. Deep-sea Sponge Grounds: Reservoirs of Biodiversity. UNEP-WCMC
436 Biodiversity Series No. 32. UNEP-WCMC, Cambridge, Uk.

437 Hosegood, P., Bonnin, J., van Haren, H., 2004a. Solibore-induced sediment resuspension in the
438 Faeroe-Shetland channel. *Geophys. Res. Lett.* 31, 2–5. <https://dx.doi.org/10.1029/2004GL019544>

439 Hosegood, P.J., van Haren, H., 2004b. Near-bed solibores over the continental slope in the Faeroe-
440 Shetland channel. *Deep-Sea Res. II* 51, 2943-2971

441 Hosegood, P. J., van Haren, H., 2006. Sub-inertial modulation of semi-diurnal currents over the
442 continental slope in the Faeroe-Shetland Channel. *Deep-Sea Res. I* 53, 627-655.

443 Howell, K.L., Davies, J.S., 2010. Deep-sea species image catalogue. Marine Biology and Ecology
444 Research Centre, Marine Institute at the University of Plymouth. On-line version:
445 <http://www.marlin.ac.uk/deep-sea-species-image-catalogue/>

446 Howell, K.L., Davies, J.S., Narayanaswamy, B.E., 2010. Identifying deep-sea megafaunal epibenthic
447 assemblages for use in habitat mapping and marine protected area network design. *J. Mar. Biol.*
448 *Assoc. U. K.* 90, 33-68. <https://doi.org/10.1017/S0025315409991299>

449 Howell, K.L., Piechaud, N., Downie, A.L., Kenny, A., 2016. The distribution of deep-sea sponge
450 aggregations in the North Atlantic and implications for their effective spatial management. *Deep-Sea*
451 *Res. I*, 115, 309-320. <https://doi.org/10.1016/j.dsr.2016.07.005>

452 Jacobs, C.L., Howell, K.L., 2007. MV Franklin Cruise 0206, 03-23 Aug 2006. Habitat investigations
453 within the SEA4 and SEA7 areas of the UK continental shelf. Southampton, UK, National

454 Oceanography Centre Southampton, 95pp. (National Oceanography Centre Southampton Research
455 and Consultancy Report 24).

456 Krautter, M., Conway, K.W., Barrie, J.V., Neuweiler, M., 2001. Discovery of a ‘living dinosaur’:
457 globally unique modern hexactinellid sponge reefs off British Columbia, Canada. *Facies* 44, 265–282.
458 <https://dx.doi.org/10.1007/BF02668178>

459 Klitgaard, A.B., Tendal, O.S., Westerberg, H., 1997. Mass occurrences of large-sized sponges
460 (Porifera) in Faroe Island (NE-Atlantic) shelf and slope areas: characteristics, distribution and
461 possible causes. In: *The Responses of Marine Organisms to their Environments*, 129–142. Ed. by
462 A.C. Jensen, M. Shbeader, and J.A. Williams. *Proceedings of the 30th European Marine Biology*
463 *Symposium*, University of Southampton.

464 Klitgaard, A.B., Tendal, O.S., 2001. “Ostur” - “cheese bottoms” - sponge dominated areas in Faroese
465 shelf and slope areas. In: Bruntse G, Tendal OS, editors. *Marine Biological Investigations and*
466 *Assemblages of Benthic Invertebrates from the Faroe Islands. The Faroe Islands: Kaldbak Marine*
467 *Biological Laboratory*. 13-21.

468 Klitgaard, A.B., Tendal, O.S., 2004. Distribution and species composition of mass occurrences of
469 large-sized sponges in the northeast Atlantic. *Prog. Oceanogr.* 61, 57–98.
470 <https://dx.doi.org/10.1016/j.pocean.2004.06.002>

471 Knudby, A., Kenchington, E., Murillo, F.J., 2013. Modeling the distribution of *Geodia* sponges and
472 sponge grounds in the Northwest Atlantic. *PloS One*, 8(12): e82306.
473 <https://doi.org/10.1371/journal.pone.0082306>

474 Kutti, T., Bannister, R., Fosså, J., 2013. Community structure and ecological function of deep-water
475 sponge grounds in the Traenadypet MPA—Northern Norwegian continental shelf. *Cont. Shelf Res.*
476 69, 21-30. <https://doi.org/10.1016/j.csr.2013.09.011>

477 Kutti, T., Bannister, R.J., Fosså, J.H., Krogness, C.M., Tjensvoll, I., Søvik, G., 2015. Metabolic
478 responses of the deep-water sponge *Geodia barretti* to suspended bottom sediment, simulated mine
479 tailings and drill cuttings. *J. Exp. Mar. Biol. Ecol.* 473, 64-72.

480 Masson, D.G., 2001. Sedimentary processes shaping the eastern slope of the Faeroe-Shetland
481 Channel, *Cont. Shelf Res.* 21, 825-857. [https://doi.org/10.1016/S0278-4343\(00\)00115-1](https://doi.org/10.1016/S0278-4343(00)00115-1)

482 Murillo, F.J., Kenchington, E., Tompkins, G., Beazley, L., Baker, E., Knudby, A., Walkusz, W., 2018.
483 Sponge assemblages and predicted archetypes in the eastern Canadian Arctic. *Mar. Ecol. Prog. Ser.*
484 597, 15-135.

485 Nansen, F., 1902. The oceanography of the north polar basin. The Norwegian North Polar Expedition,
486 1893-1896, Scientific Results, Longmans, Green & Co., vol. 3, 427.

487 R Core Team, 2016. R: A language and environment for statistical computing. R Foundation for
488 Statistical Computing, Vienna, Austria. URL <https://www.R-project.org/>

489 Reiswig, H.M., 1975. Bacteria as food for temperate-water marine sponges. *Can. J. Zool.* 53, 582-589.

490 Rice, A.L., Thurston, M.H., New, A., 1990. Dense aggregations of a hexactinellid sponge, *Pheronema*
491 *carpenteri*, in the Porcupine Seabight (northeast Atlantic Ocean), and possible causes. *Prog.*
492 *Oceanogr.* 24, 179–196. [https://dx.doi.org/10.1016/0079-6611\(90\)90029-2](https://dx.doi.org/10.1016/0079-6611(90)90029-2)

493 Roberts, E.M., Mienis, F., Rapp, H.T., Hanz, U., Meyer, H.K., Davies, A.J., 2018. Oceanographic
494 setting and short-timescale environmental variability at an Arctic seamount sponge ground. *Deep-Sea*
495 *Res. I.* 138, 98-113. <https://doi.org/10.1016/j.dsr.2018.06.007>

496 Ross, R.E., Howell, K.L., 2013. Use of predictive habitat modelling to assess the distribution and
497 extent of the current protection of “listed” deep-sea habitats. *Divers. Distrib.* 19, 433–445.
498 <https://dx.doi.org/10.1111/ddi.12010>

499 Tjensvoll, I., Kutti, T., Fosså, J.H., Bannister, R.J., 2013. Rapid respiratory responses of the deep-
500 water sponge *Geodia barretti* exposed to suspended sediments. *Aquat. Biol.* 19, 65–73.
501 <https://dx.doi.org/10.3354/ab00522>

502 Turrell, W.R., Slesser, G., Adams, R.D., Payne, R., Gillibrand, P.A., 1999. Decadal variability in the
503 composition of Faroe Shetland Channel bottom water. *Deep-Sea Res. I* 46, 1–25.
504 [https://dx.doi.org/10.1016/S0967-0637\(98\)00067-3](https://dx.doi.org/10.1016/S0967-0637(98)00067-3)

505 UNGA., 2006. Resolution 61/105. Sustainable fisheries, including through the 1995 Agreement for
506 the Implementation of the Provisions of the United Nations Convention on the Law of the sea of 10
507 December 1982 relating to the conservation and management of straddling fish Stocks and highly
508 migratory fish stocks, and related instruments. UNGA A/RES/61/105.

509 van Haren, H., Cimadoribus, A., Gostiaux, L., 2015. Where large deep-ocean waves break. *Geophys.*
510 *Res. Lett.* 42, 2351-2357. doi:10.1002/2015GL063329.

511 van Haren, H., Hanz, U., de Stigter, H., Mienis, F., Duineveld, G., 2017. Internal wave turbulence at a
512 biologically rich Mid-Atlantic seamount. *PLoS One*, 12(12), e0189720.
513 <https://doi.org/10.1371/journal.pone.0189720>

514 Van Raaphorst, W., Malschaert, H., Van Haren, H., 2001. Cross-slope zonation of erosion and
515 deposition in the Faeroe-Shetland Channel, North Atlantic Ocean. *Deep-Sea Res. I* 48, 567–591.
516 [https://dx.doi.org/10.1016/S0967-0637\(00\)00052-2](https://dx.doi.org/10.1016/S0967-0637(00)00052-2)

517 Van Soest, R.W., Boury-Esnault, N., Vacelet, J., Dohrmann, M., Erpenbeck, D., de Voogd, N.J.,
518 Santodomingo, N., Vanhoorne, B., Kelly, M., Hooper, J.N., 2012. Global diversity of sponges
519 (Porifera). *PLoS One*, 7(4): e35105. <https://doi.org/10.1371/journal.pone.0035105>

520 Vogel, S., 1977. Current-induced flow through living sponges in nature. *Proc. Natl. Acad. Sci. U.S.A.*
521 74, 2069–2071. <https://dx.doi.org/10.1073/pnas.74.5.2069>

522 White, M., 2003. Comparison of near seabed currents at two locations in the Porcupine Sea Bight
523 implications for benthic fauna. *J. Mar. Biol. Assoc. U. K.* 83, 683–686. <https://doi.org/10.1017/S0025>

524 Yahel, G., Sharp, J.H., Marie, D., Häse, C., Genin, A., 2003. In situ feeding and element removal in
525 the symbiont-bearing sponge *Theonella swinhoei*: Bulk DOC is the major source for carbon. *Limnol.*
526 *Oceanogr.* 48, 141-149.

The distribution of deep-sea sponge aggregations (Porifera) in relation to oceanographic processes in the Faroe-Shetland Channel.

Joshua J. Davison, Hans van Haren, Phil Hosegood, Nils Piechaud, Kerry L. Howell.

Supplementary material

Figure S1: Temperature profiles generated from 36 CTD casts in the Faroe-Shetland Channel, temperature range was calculated in 20m depth bins.

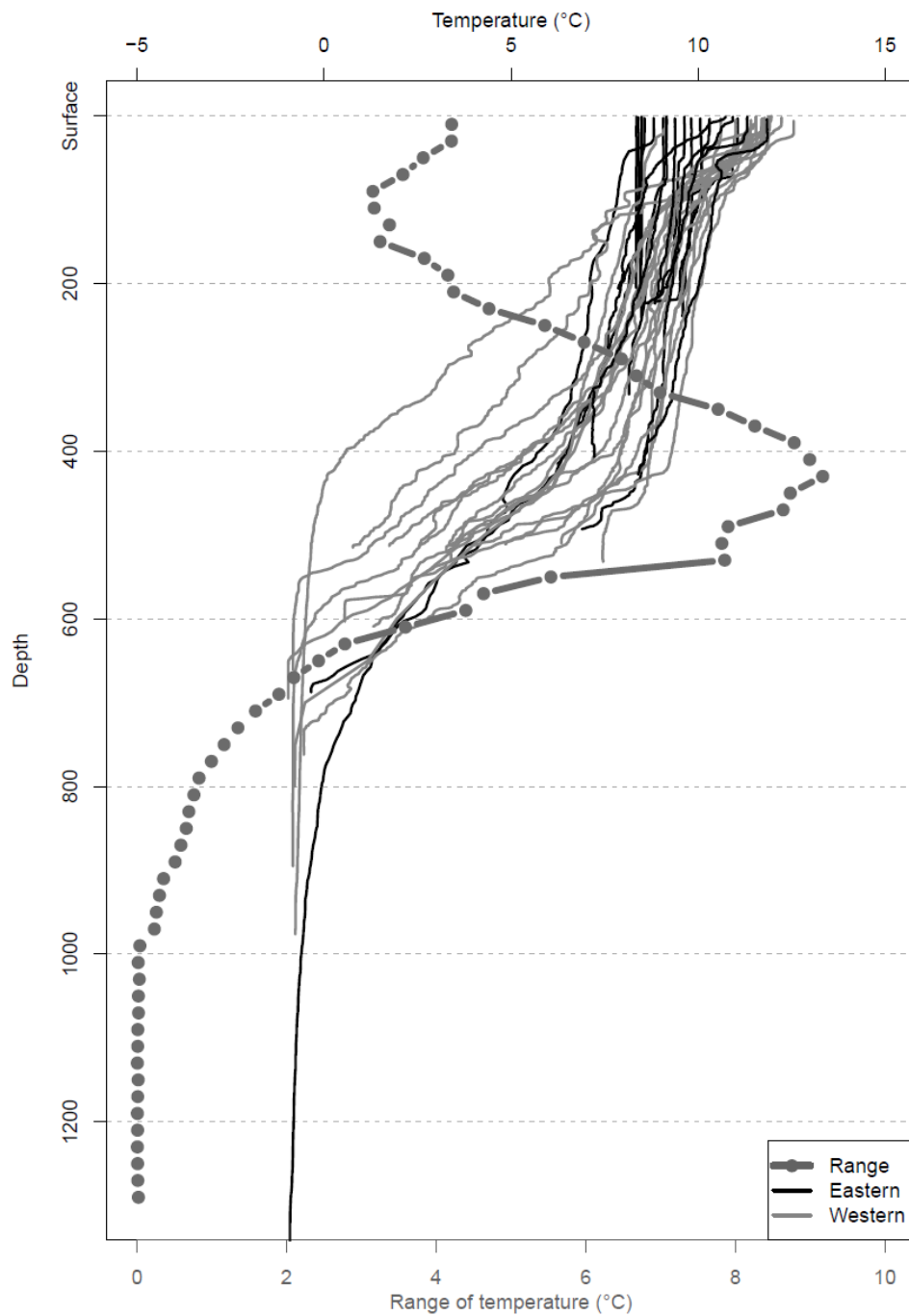
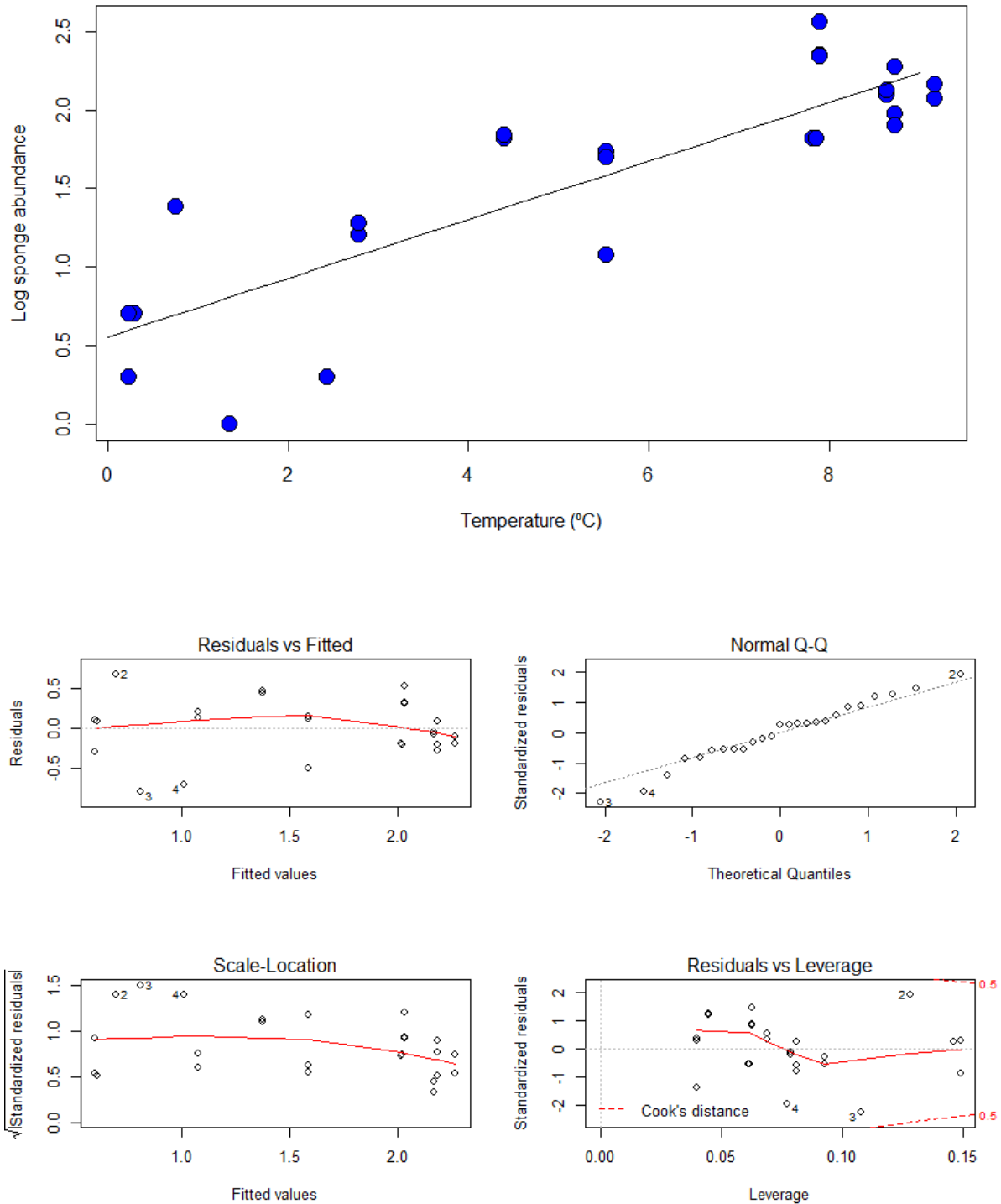


Figure S2: a) linear regression of log sponge abundance vs CTD temperature range.
 b) diagnostic plots



Raw model output

```
lm(formula = logAbunP1 ~ TempR, data = data)
```

Residuals:

Min	1Q	Median	3Q	Max
-0.80616	-0.20192	0.08876	0.20566	0.68389

Coefficients:

	Estimate	Std. Error	t value	Pr(> t)	
(Intercept)	0.55398	0.14929	3.711	0.00115	**
TempR	0.18680	0.02348	7.955	4.72e-08	***

Signif. codes: 0 '***' 0.001 '**' 0.01 '*' 0.05 '.' 0.1 ' ' 1

Residual standard error: 0.375 on 23 degrees of freedom
 Multiple R-squared: 0.7334, Adjusted R-squared: 0.7219
 F-statistic: 63.29 on 1 and 23 DF, p-value: 4.722e-08

Figure S3: a) Box plots showing mean sponge abundance vs long term OBS from 3 moorings deployed at different depths on the slope (PROCS-2). Low obs = 0.088 v, mooring depth 1043m, Med= 0.092 v, mooring depth 803m. High = 0.198 v, mooring depth 552m

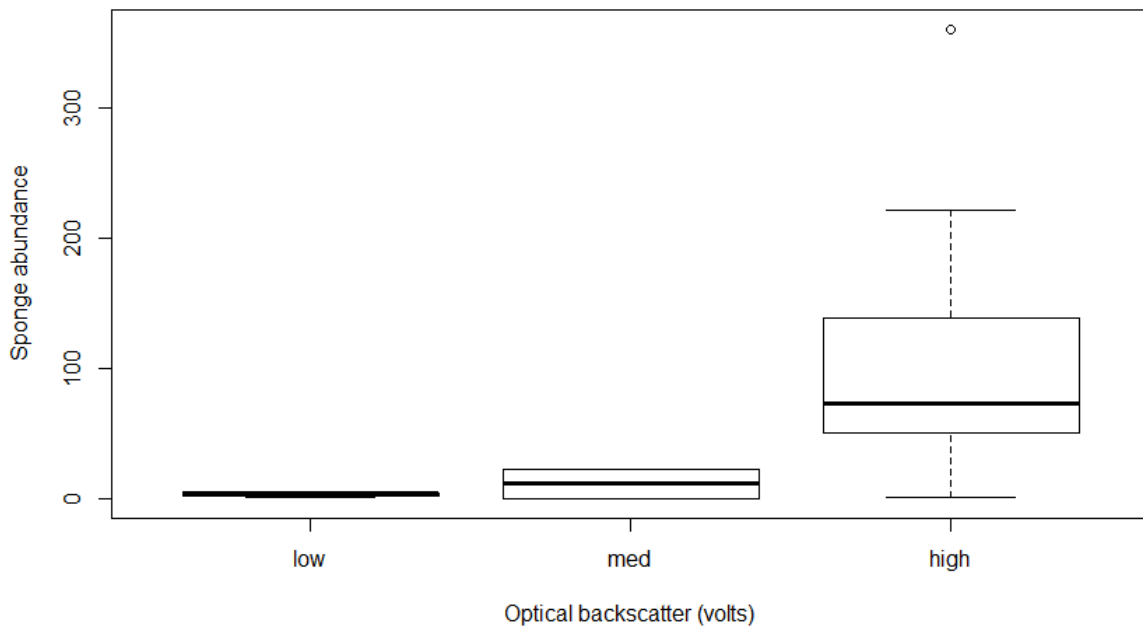


Figure S4: Sponge abundance determined from pooled image data by transect, temperature range from CTD casts, and seasonal short term optical backscatter (PROCS-1 & 3) as a function of depth.

